

# Intelligent swarm-based optimization technique for oscillatory stability assessment in power system

N. A. M. Kamari<sup>1</sup>, I. Musirin<sup>2</sup>, A. A. Ibrahim<sup>3</sup>, S. A. Halim<sup>4</sup>

<sup>1,3,4</sup>Centre for Integrated Systems Engineering and Advanced Technologies (INTEGRA), Faculty of Engineering and Built Environment, Universiti Kebangsaan Malaysia, 43600 Bangi, Selangor, Malaysia

<sup>1,3,4</sup>Electrical and Electronic Engineering Program, Faculty of Engineering and Built Environment, Universiti Kebangsaan Malaysia, 43600 Bangi, Selangor, Malaysia

<sup>2</sup>Faculty of Electrical Engineering, Universiti Teknologi Mara, 40450 Shah Alam, Selangor, Malaysia

## Article Info

### Article history:

Received Aug 9, 2019

Revised Oct 23, 2019

Accepted Nov 6, 2019

### Keywords:

Angle stability

Damping ratio

Damping torque coefficients

Eigenvalue

Particle swarm optimization

## ABSTRACT

This paper discussed the prediction of oscillatory stability condition of the power system using a particle swarm optimization (PSO) technique. Indicators namely synchronizing ( $K_s$ ) and damping ( $K_d$ ) torque coefficients is appointed to justify the angle stability condition in a multi-machine system. PSO is proposed and implemented to accelerate the determination of angle stability. The proposed algorithm has been confirmed to be more accurate with lower computation time compared with evolutionary programming (EP) technique. This result also supported with other indicators such as eigenvalues determination, damping ratio and least squares method. As a result, proposed technique is achievable to determine the oscillatory stability problems.

Copyright © 2019 Institute of Advanced Engineering and Science.  
All rights reserved.

### Corresponding Author:

Nor Azwan Mohamed Kamari,

Electrical and Electronic Engineering Program,

Faculty of Engineering and Built Environment,

Universiti Kebangsaan Malaysia, 43600 Bangi, Selangor, Malaysia.

Email: azwank@ukm.edu.my

## 1. INTRODUCTION

With the increase of energy consumption in this age, a study on the stability of the power system becomes a necessity, especially the oscillatory stability analysis of power systems. This analysis is used to predict electromagnetic swing at low frequencies as a result of undisturbed rotor swing. References [1-10] pointed out that the stability of the oscillation in the power system is an important issue. As the power system operation changes over time, the stability of the small signal in this power system should be tracked online. Selected stability indicators are calculated from the data provided over time to track the system. These indicators are updated until a constant value is obtained. In this study, damping torque coefficient  $K_d$  and synchronizing torque coefficient  $K_s$  are used as stability indicators. Both  $K_s$  and  $K_d$  values must be positive so that the system can be classified as stable [8-10].

The least squares (LS) method is a technique commonly used to find the  $K_s$  and  $K_d$  values, as reported in [8-10]. However, data update requirements are a major weakness of the LS method. In addition, this technique also requires a long computation time. Due to these problems, the LS method requires monitoring throughout the duration of the swing. Computational intelligence methods are generally used to solve problems in power system stability. Optimisation methods include artificial neural network (ANN) [11-13], Genetic Algorithm (GA) [14-16], evolutionary programming (EP) [17-21] and Artificial Immune Systems (AIS) [22-24]. ANN is the processing systems that inspired by biological neural networks that make up the animal brains. Such systems can learn to perform tasks by considering the

examples given. On the other hand, GA is a search technique in which the application is based on the combination of natural selection and genetic mechanisms. Major characteristic in GA is the crossover and mutation operations which able it to produce high quality solution. The set back of GA is it took too long time to converge. Meanwhile, EP and AIS are heuristic population-based search methods that used random variation, mutation and selection. Something that distinguishes them is AIS also highlighted a process called cloning. This paper discussed a new heuristic approach named Particle Swarm Optimization (PSO) technique [25-29]. PSO is influenced by the behaviours of schools of fish and flocks of birds. It shows performance beyond EP, AIS and GA methods in searching the optimal solution with faster computation time.

This paper proposes an efficient technique for estimating synchronizing and damping torque coefficients in solving oscillatory stability problems. Using this technique,  $K_s$  and  $K_d$  values are estimated based on information by three generator responses, namely, the changes in rotor speed ( $\Delta\omega(t)$ ), the changes in rotor angle ( $\Delta\delta(t)$ ) and the changes in electromechanical torque ( $\Delta T_e(t)$ ). The goal is to minimize the error of the estimated coefficients. The IEEE 30-Bus system has been chosen to test the online estimation technique for  $K_s$  and  $K_d$ . This paper discussed the oscillatory stability prediction in a multi-machine system using PSO. A mathematical model for IEEE 30-Bus system for the angle stability assessment is developed. PSO is chosen to optimize the objective function, with  $J$  as well as  $K_s$  and  $K_d$  as the control variables. Once the  $J$  value has been maximized,  $K_s$  and  $K_d$  are analyzed, which verify the stability condition of the system. The performance of PSO is then compared with EP and LS. Results obtained from the experiment are then verified with the minimum damping ratio ( $\zeta_{min}$ ) [30-32] and eigenvalues ( $\lambda$ ).

## 2. IMPLEMENTATION OF ANGLE STABILITY ANALYSIS

The IEEE 30-Bus system model is selected to demonstrate the potential of the proposed technique in angle stability assessment for a multi-machine system. Six generators, namely, Generators 1, 2, 5, 8, 11 and 13 are connected to the buses named Buses 1, 2, 5, 8, 11 and 13, respectively. Reference [9] shows the parameters of the system.

### 2.1. Philips-heffron model for multi-machine system

The proposed Phillips-Heffron model for the multi machine system is developed and shown in Figure 1. The model is developed on the basis of the single machine of the Phillips-Heffron model [10].  $K_d$  is the damping torque coefficient,  $H$  is the inertia constant,  $T_A$  and  $K_A$  are the time constant and circuit constant of the exciter, respectively.  $\omega_0$  is equal to  $2\pi f_0$ .  $K_1-K_6$  and  $T_3$  are constants that consist of the function related to the operating real and reactive loading, impedance, electrical torque, and the excitation levels in the generator.

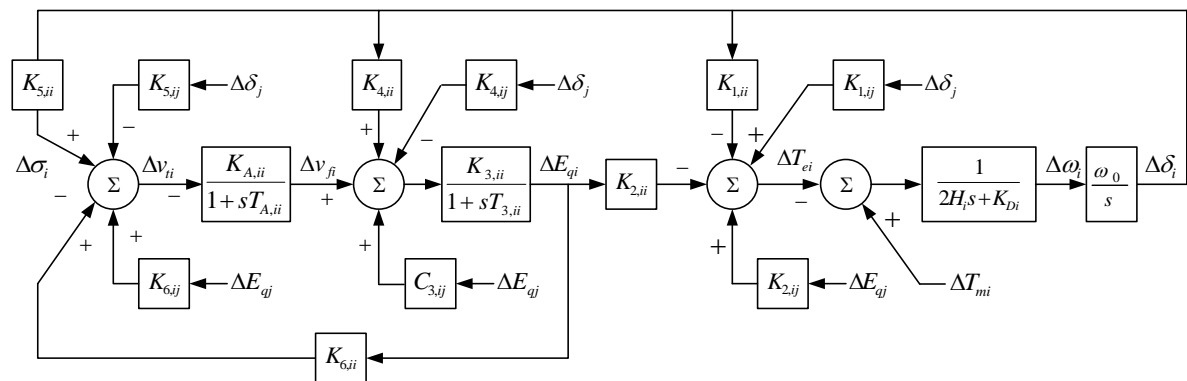


Figure 1. Phillips-heffron model for multi-machine system

### 2.2. Mathematical modelling of philips-heffron model

Mathematical modelling can be derived for the proposed Phillips-Heffron model for the multi machine system shown in Figure 1 and is presented in the following mathematical equations:

$$\Delta\omega_i/\Delta t = (\Delta T_{mi} - \Delta T_{ei} - K_{Di}\Delta\omega_i)/2H_i, i = 1, \dots, m \quad (1)$$

$$\Delta\delta_i/\Delta t = \omega_0\Delta\omega_i, i = 1, \dots, m \quad (2)$$

$$\begin{aligned} \Delta E_{qi}/\Delta t = & \left( K_{4,ii}\Delta\delta_i - \sum_{j \neq i} K_{4,ij}\Delta\delta_j - C_{3,ii}\Delta E'_{qi} \right) / \Delta T'_{d0i}, \quad i = 1, \dots, m, \quad j = 1, \dots, m, \quad i \neq j \\ & + \sum_{j \neq i} C_{3,ij}\Delta E'_{qj} + \Delta v_{fi} \end{aligned} \quad (3)$$

$$\Delta v_{fi}/\Delta t = \left( \begin{array}{l} -K_{5,ii}\Delta\delta_i + \sum_{j \neq i} K_{5,ij}\Delta\delta_j \\ -K_{6,ii}\Delta E'_{qi} + \sum_{j \neq i} K_{6,ij}\Delta E'_{qj} \end{array} \right) / T_{Ai} - \Delta v_{fi}/\Delta T_{Ai}, \quad i = 1, \dots, m, \quad j = 1, \dots, m, \quad i \neq j \quad (4)$$

$$\Delta T_{ei} = \left( \begin{array}{l} K_{1,ii}\Delta\delta_i - \sum_{j \neq i} K_{1,ij}\Delta\delta_j \\ + K_{1,ii}\Delta E'_{qi} - \sum_{j \neq i} K_{2,ij}\Delta E'_{qj} \end{array} \right), \quad i = 1, \dots, m, \quad j = 1, \dots, m, \quad i \neq j \quad (5)$$

Reference [3] showed the details on (1-5). Can be rewritten into matrix form as follows:

$$\dot{X}_i = A_i \cdot X_i + B_i \cdot U_i, i = 1, \dots, m \quad (6)$$

$$X_i = [\Delta\omega_i \quad \Delta\delta_i \quad \Delta E_{qi} \quad \Delta v_{fi}]^T, i = 1, \dots, m \quad (7)$$

$$U_i = [\Delta T_{ei}], i = 1, \dots, m \quad (8)$$

$U_i$  and  $X_i$  are the input and state signal vectors for  $i$  generators, respectively.  $A_i$  is the system parameters' function with  $i$  generators.  $B_i$  is the disturbance matrix.

### 2.3. Synchronizing and damping torque coefficients

The correlation between the change in estimated electromagnetic torque deviation ( $\Delta T_{esi}(t)$ ) and the changes in rotor angle ( $\Delta\delta_i(t)$ ) and rotor speed ( $\Delta\omega_i(t)$ ) for the  $i$ th generator can be expressed as follows:

$$\Delta T_{esi}(t) = K_{si}\Delta\delta_i(t) + K_{di}\Delta\omega_i(t), i = 1, \dots, m \quad (9)$$

where  $K_{si}$  and  $K_{di}$  are  $K_s$  and  $K_d$  for the  $i$ th generator, respectively, and  $m$  is the number of generators. The justification of the stability of a linear system can be performed via the estimation of  $K_s$  and  $K_d$ . The positive values of  $K_s$  and  $K_d$  will validate the system as stable. If the system has positive  $K_s$  and negative  $K_d$ , then it is defined to be in the oscillatory instability condition. However, if  $K_s$  and  $K_d$  indicate negative and positive values, respectively, then the system is considered to be in the non-oscillatory instability condition. In general, the system is unstable if either one of the torque coefficients is negative.

The stability evaluation of a linear system can be predicted with reference to the  $K_s$  and  $K_d$  values. A stable system is guaranteed if the  $K_s$  and  $K_d$  values are positive. If the linear system has positive  $K_s$  and negative  $K_d$ , then the system is defined to be in the oscillatory instability condition. The effect of the oscillatory instability condition can be detected from the increment of the amplitude oscillations of the rotor. Non-oscillatory instability occurs if  $K_s$  and  $K_d$  show negative and positive values, respectively. This condition can be verified from the steady increment of rotor angle responses. Detail illustration of stable, oscillatory unstable and non-oscillatory unstable conditions can be found in [1].

### 2.4. Eigenvalues and damping ratio

The scalar parameter of eigenvalues,  $\lambda$  can be derived as follows [1]:

$$(A - \lambda I)\varphi = 0 \quad (10)$$

Here, the  $n$  solutions of  $\lambda$  ( $=\lambda_1, \lambda_2, \dots, \lambda_n$ ) are the eigenvalues of  $A$ . The  $i^{\text{th}}$  eigenvalue can be stated as follows:

$$\lambda_i = \sigma_i \pm j\omega_i \quad (11)$$

where  $\sigma_i$  and  $\omega_i$  are the real and the imaginary part of the  $i^{\text{th}}$  eigenvalue, respectively. If all value of  $\lambda$  have negative real parts, the linear system is considered stable. The damping ratio ( $\xi_i$ ) for the  $i^{\text{th}}$  eigenvalue is defined as the following:

$$\xi_i = -\sigma_i / \sqrt{\sigma_i^2 + \omega_i^2} \quad (12)$$

The linear system is certainly in stable condition if all damping ratio have positive value. For simplification purposes, only the minimum value of the damping ratio, ( $\zeta_{min}$ ) for the linear system is selected to verify the result [30-32].

## 2.5. LS method

LS technique is often used to obtain the minimum value for the sum of the square of the differences between  $\Delta T_e(t)$  and  $\Delta T_{es}(t)$ . The error is defined as [8-10]:

$$E(t) = \Delta T_e(t) - \Delta T_{es}(t) \quad (13)$$

Here,  $\Delta T_e(t)$  and  $\Delta T_{es}(t)$  are the real and estimated electrical torque, respectively.

The period of  $t_{total}$  must be chosen to estimate the correct value for  $K_s$  and  $K_d$ . The different values of  $t_{total}$  will result in an inaccurate value for  $K_s$  and  $K_d$ . References [8] stated that the suitable value for  $t_{total}$  that makes  $K_s$  and  $K_d$  constant during the oscillation period is the value of the entire oscillation period. In matrix notation, the problem can be described as follows:

$$\Delta T_e(t) = \Delta T_{es}(t) + E(t) = Cx + E(t) \quad (14)$$

$$C = [\Delta\delta(t) \quad \Delta\omega(t)] \quad (15)$$

$$x = [K_s \quad K_d]^T \quad (16)$$

Here  $\Delta T_e(t)$  and  $\Delta T_{es}(t)$  are the real and estimated electrical torque, respectively.  $E(t)$  is the differences (error) between  $\Delta T_e(t)$  and  $\Delta T_{es}(t)$ . Detail calculations can be found in [10]. Although the calculated values are accurate, the application of the LS method requires a full oscillation period and takes a long time [8]. Therefore, a new indicator is necessary.

## 3. OPTIMIZATION TECHNIQUES

Nowadays, artificial intelligence technology (AI) has been widely used in solving power system problems. Evolutionary computation (EC) is one of the AI techniques that promotes logical representation approaches. EC is a group of global optimization algorithms that has metaheuristic optimization properties. Inspired by biological evolution, among the techniques covered in EC are EP, GA, AIS and PSO. EP and PSO are selected as optimization techniques in the present study.

### 3.1. PSO

The PSO algorithm is started with initialization, followed by the update of velocity and position, fitness calculation, the best position update and convergence test. Detailed explanations of PSO algorithm process are as followed.

#### 3.1.1. Initialization

In the initialization process of PSO, the value of synchronizing and damping torque coefficient,  $K_s$  and  $K_d$  are generated randomly. In the PSO perspective,  $K_s$  and  $K_d$  are called particles and their values are called position (or  $x$ ). For every position that is created,  $x_i$ , there is a velocity,  $v_i$ . In the initialization process, the velocity is also randomly created in the range [0, 1]. The random positions are then used to calculate the fitness,  $J$ . In this initialization process, the  $i^{th}$  fitness,  $J_i$  is set as individual best fitness  $J_{i,p}$  for  $i^{th}$  particle. For the  $K_s$  and  $K_d$  estimation process, one constraint is identified: the calculated  $J$  must be larger than 0.5. Initialization process is repeated until total number of initial particles,  $n$  is achieved. From these  $N$  set of particles, the maximum fitness of all particles,  $J_{max}$  is set as the global best fitness,  $J_g$ . The position for every  $J_{i,p}$ ,  $J_{max}$  and  $J_g$  is set respectively as the individual best position  $p_i$ , position with maximum fitness  $p_{max}$  and global best position  $p_g$ .

#### a. Velocity and position update

After set of particles are selected in initialization level, all  $n$  particles are through a process of updating the velocity and position, for every particle. The update process of  $v_i$  and  $x_i$  for the  $i^{th}$  particle at  $j^{th}$  iteration is in line with the following equations:

$$v_i(j) = \omega v_i(j-1) + c_1\{p_i(j-1) - x_i(j-1)\} + c_2\{g(j-1) - x_i(j-1)\} \quad (17)$$

$$x_i(j) = v_i(j) + x_i(j-1) \quad (18)$$

Here,  $c_1$  and  $c_2$  are acceleration coefficients and  $\omega$  is the inertia weight.

#### b. Fitness calculation

Using the new value of  $v_i$  and  $x_i$ , the new fitness,  $J_i$  are calculated for every new  $n$  particles. After new fitness is calculated, new value of  $J_{max}$  and the minimum fitness of all particles,  $J_{min}$  are selected.

#### c. Best position update

With the new set of position, velocity and fitness for  $n$  particles, the update process of individual best position,  $p_i$  and the global best position,  $p_g$  will be performed if the following conditions are met:

- If  $J_i$  is bigger than  $J_{i,p}$ , select  $J_i$  as  $J_{i,p}$ , and select  $x_i$  as  $p_i$ . If  $J_i$  is smaller than or equal with  $J_{i,p}$ , the value of  $J_{i,p}$  and  $p_i$  are not changed.
- If  $J_{max}$  is bigger than  $J_g$ , select  $J_{max}$  as  $J_g$ , and select  $p_{max}$  as  $p_g$ . Else, if  $J_{max}$  is smaller than or equal with  $J_g$ , the value of  $J_g$  and  $p_g$  are not changed.

#### d. Convergence test

Convergence test is attended to regulate the stopping criteria of the optimization process. The search process will be terminated if the process has reached the maximum iteration number or the difference between the value of  $J_{max}$  and  $J_{min}$  is very close to 0. The flow chart which represents the PSO algorithm is illustrated in Figure 2(a).

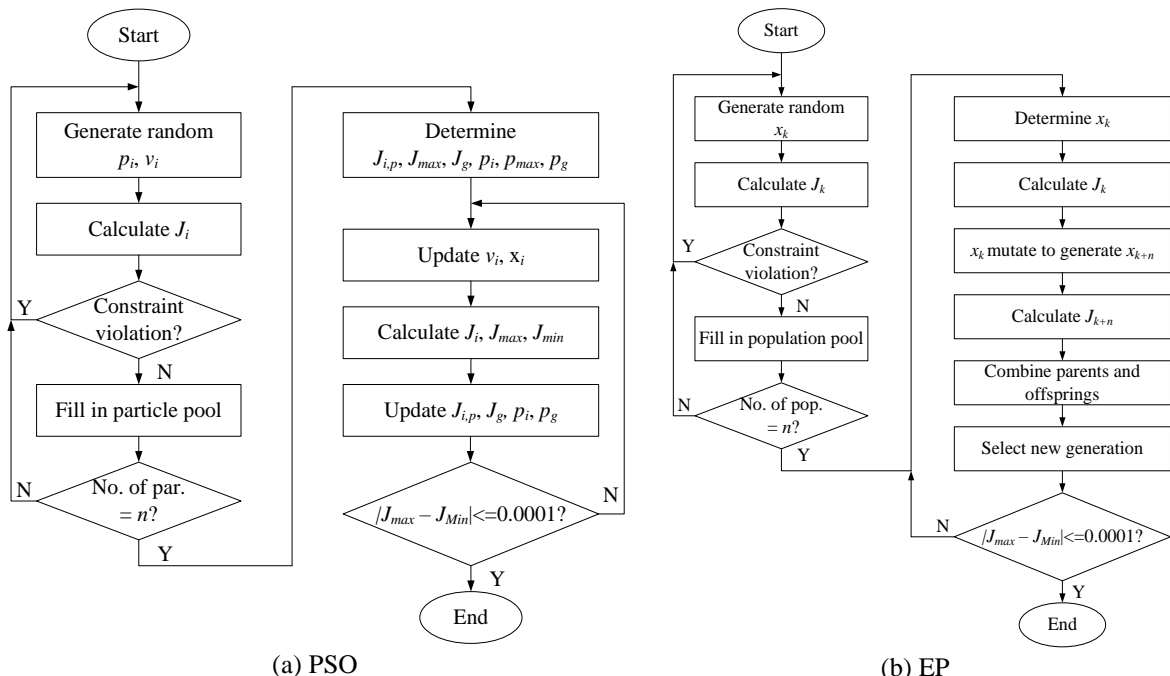


Figure 2. Algorithm flowchart

### 3.2. EP

The Evolutionary Programming (EP) is inspired by the theory of evolution based on natural selection. Metaphorically, the breeding of a species will produce offspring with some small variations due to mutations. With the competition between offspring and parents in finding the suitability of the environment, more suitable members will be chosen next generation. This new generation will reproduce, and this process repeats until the suitability between the species and the environment is reached. The overall process of EP algorithm is illustrated in Figure 2(b). Detailed explanations of EP algorithm process can be found in [10].

### 3.3. Objective functions

In the current study, the objective function formulated is based on the differences of the electromagnetic and estimated electromagnetic torques of the  $i^{\text{th}}$  generator,  $\Delta T_{ei}(t)$  and  $\Delta T_{esi}(t)$ , respectively, as depicted in (21). This difference or error is estimated for the calculation of  $K_s$  and  $K_d$  for every generator in the system. The PSO optimization technique is used to minimize the error with  $K_s$  and  $K_d$  being the control variables [10].

$$J_i = \text{inv} \left( 1 + \text{abs} \left( (\Delta T_{ei}(t) - \Delta T_{esi}(t)) / \Delta T_{ei}(t) \right) \right), i = 1, \dots, m \quad (19)$$

where  $m$  is the number of generators. Hence, the objective function can be defined as follows:

Maximize ( $J_i$ )

From the optimized  $J$  value, a decision can be made to identify the angle stability on the basis of the  $K_s$  and  $K_d$  values.

### 3.4. Algorithm for angle stability assessment

The calculation process of  $K_{si}$  and  $K_{di}$  for the  $i^{\text{th}}$  generator is conducted repeatedly to estimate successfully the maximum value of  $J_i$ . The following process is implemented:

- Calculate  $\Delta T_{esi}(t)$  using  $\Delta \delta_i(t)$ ,  $\Delta \omega_i(t)$ , and the estimated torque coefficients using (9).
- Evaluate  $J_i$  using (19).
- If  $J_i$  is smaller than 1.00, then vary the values of  $K_{si}$  and  $K_{di}$  and repeat steps a and b with newly generated  $\Delta \delta_i(t)$  and  $\Delta \omega_i(t)$  sample data until  $J_i$  reaches 1.00 or all sample data are used.

Table 1 tabulates the parameters used in EP and PSO optimization process.

Table 1. Parameters of EP and PSO

| Techniques | EP             | PSO               |
|------------|----------------|-------------------|
| Parameters | $\beta = 0.09$ | $c_1 = c_2 = 0.9$ |

## 4. RESULTS AND DISCUSSION

The achievement of the PSO technique in estimating  $K_s$  and  $K_d$  are conducted via the IEEE 30-bus system. Generator data for this system can be found in [7]. Three samples of data of rotor angle  $\Delta \delta(t)$ , electrical torque  $\Delta T_e(t)$  and rotor speed  $\Delta \omega(t)$  for all six generators are produced in a MATLAB/Simulink environment. Two different values of reactive load at Bus 2 are used to simulate various stability cases. The values of the reactive load at Bus 2 are chosen in such a way that two scenarios can be emulated, namely, stable and critically unstable conditions as tabulated in Table 2. The three responses, namely angle, speed and torque deviations for Case 1 are shown in Figure 3(a), 3(b) and 3(c), respectively. In this case, the high damping rate for all responses justifies the system as in stable condition. Overall, all responses are fully damped 33 s after the simulation started.

Table 2. Two different loading conditions

| Case                   | 1 (stable condition) | 2 (critically unstable condition) |
|------------------------|----------------------|-----------------------------------|
| Reactive load at Bus 2 | 35 Mvar              | 210 Mvar                          |

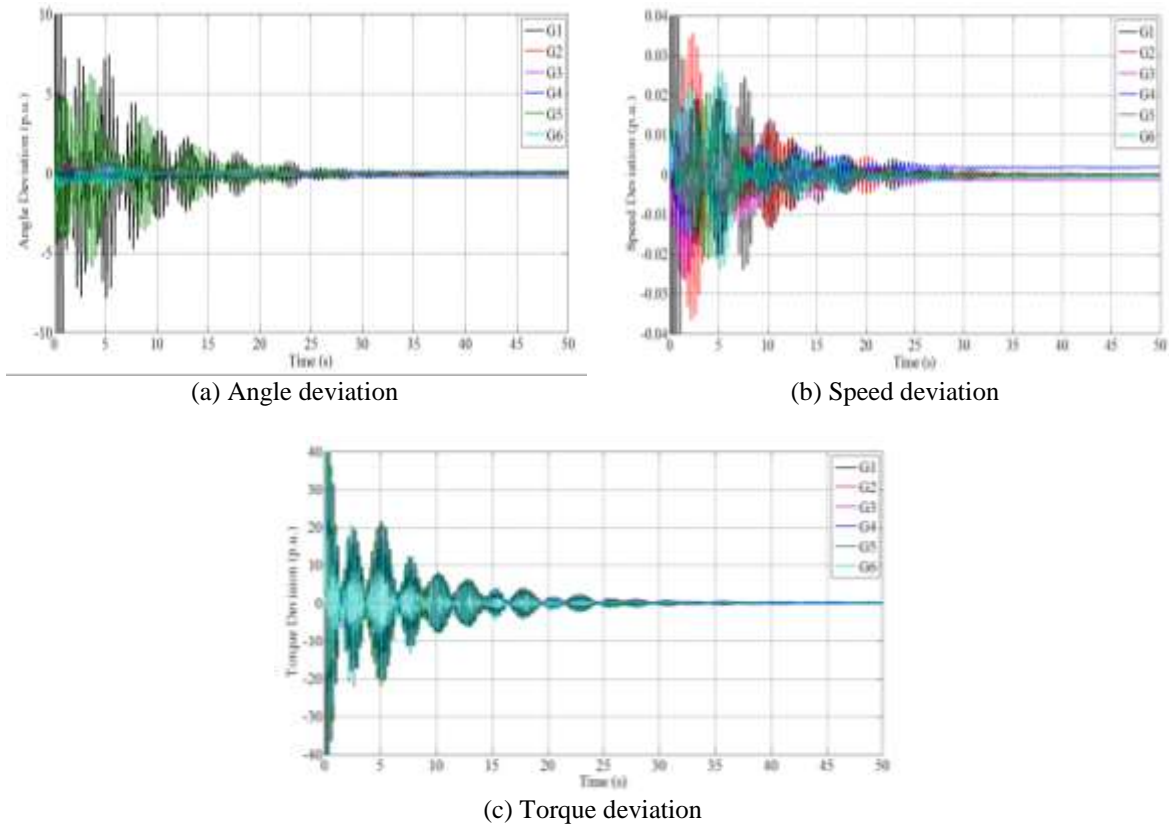


Figure 3. Responses for stable condition for all generators in case 1

Table 3 tabulates the comparison of  $K_s$ ,  $K_d$ ,  $J$  and number of iterations optimized for six different generators from EP, PSO and LS method for Case 1. All the three techniques manage to predict the stability conditions correctly indicated by the positive values of torque coefficients  $K_s$  and  $K_d$  for all the six generators. In this case, PSO method succeeds to calculate fitness value of 1.000 for all generators. On the other hand, EP calculated the highest fitness value of 0.8805 for generator G5. From the iteration perspective, PSO and EP are close to each other i.e. between 14~18 iterations. Table 4 shows the comparisons of fitness  $J$  and iteration result for Case 1. From eigenvalues  $\lambda$  perspective, all values are negative, meanwhile the minimum damping ratio  $\zeta_{min}$  give positive value. This confirms that case 1 is a stable case.

Table 3. Comparisons of EP, PSO and LS method for case 1

| Gen. | Tech. | $K_s$  | $K_d$   | $J$    | No. Iter. | Gen. | Tech. | $K_s$  | $K_d$  | $J$    | No. Iter. |
|------|-------|--------|---------|--------|-----------|------|-------|--------|--------|--------|-----------|
| G1   | EP    | 4.5152 | 6.7687  | 0.8204 | 17        | G4   | EP    | 0.3305 | 0.6409 | 0.8077 | 15        |
|      | PSO   | 3.8295 | 7.7154  | 1.000  | 14        |      | PSO   | 0.6419 | 0.8375 | 1.0000 | 18        |
|      | LS    | 3.4122 | 7.1221  | -      | -         |      | LS    | 0.5012 | 0.0819 | -      | -         |
|      | EP    | 0.0402 | 0.2196  | 0.8218 | 15        |      | EP    | 1.7562 | 6.0567 | 0.8885 | 14        |
| G2   | PSO   | 0.1063 | 0.2285  | 1.0000 | 14        | G5   | PSO   | 1.4818 | 9.1044 | 1.0000 | 14        |
|      | LS    | 0.0903 | 0.0131  | -      | -         |      | LS    | 1.1976 | 7.4533 | -      | -         |
|      | EP    | 9.1289 | 11.3642 | 0.8113 | 18        |      | EP    | 4.3506 | 3.7928 | 0.8315 | 16        |
| G3   | PSO   | 7.6795 | 9.5289  | 1.0000 | 15        | G6   | PSO   | 3.7917 | 8.6296 | 1.0000 | 16        |
|      | LS    | 6.2812 | 10.3265 | -      | -         |      | LS    | 4.0129 | 7.7373 | -      | -         |

Table 4. The results of  $\lambda$  and  $\zeta_{min}$  for case 1

| $\zeta_{min}$ | $\lambda$                                                                                                                                                                                                                                                                             |
|---------------|---------------------------------------------------------------------------------------------------------------------------------------------------------------------------------------------------------------------------------------------------------------------------------------|
| 0.0071        | $-25.3277 \pm j82.5561, -25.1949 \pm j67.3925, -25.1835 \pm j66.2373, -25.1689 \pm j64.4594,$<br>$-25.1727 \pm j65.1107, -25.1770 \pm j64.7891, -0.0321, -0.2579, -0.1240 \pm j14.6853,$<br>$-0.1257 \pm j15.4743, -0.1142 \pm j16.0849, -0.1424 \pm j17.1449, -0.1409 \pm j16.6304.$ |

Case 2 is unstable case which supported by the oscillation increment of angle, speed and torque deviation for all six generators, shown in Figure 4(a), 4(b) and 4(c), respectively. Case 2 seems to damp in the first place, but after the simulation achieved in 15 seconds, the oscillation of the responses increasing dramatically until the simulation end. If analyzing the angle, speed or torque responses in short time i.e. 10-15 s, this case can be considered as a stable case. Unfortunately, if analyzing these three responses in 50 s and above, the oscillations seems increasing gradually and obviously the damping will not stop. Based on these results, Case 2.2B is considered as unstable case.

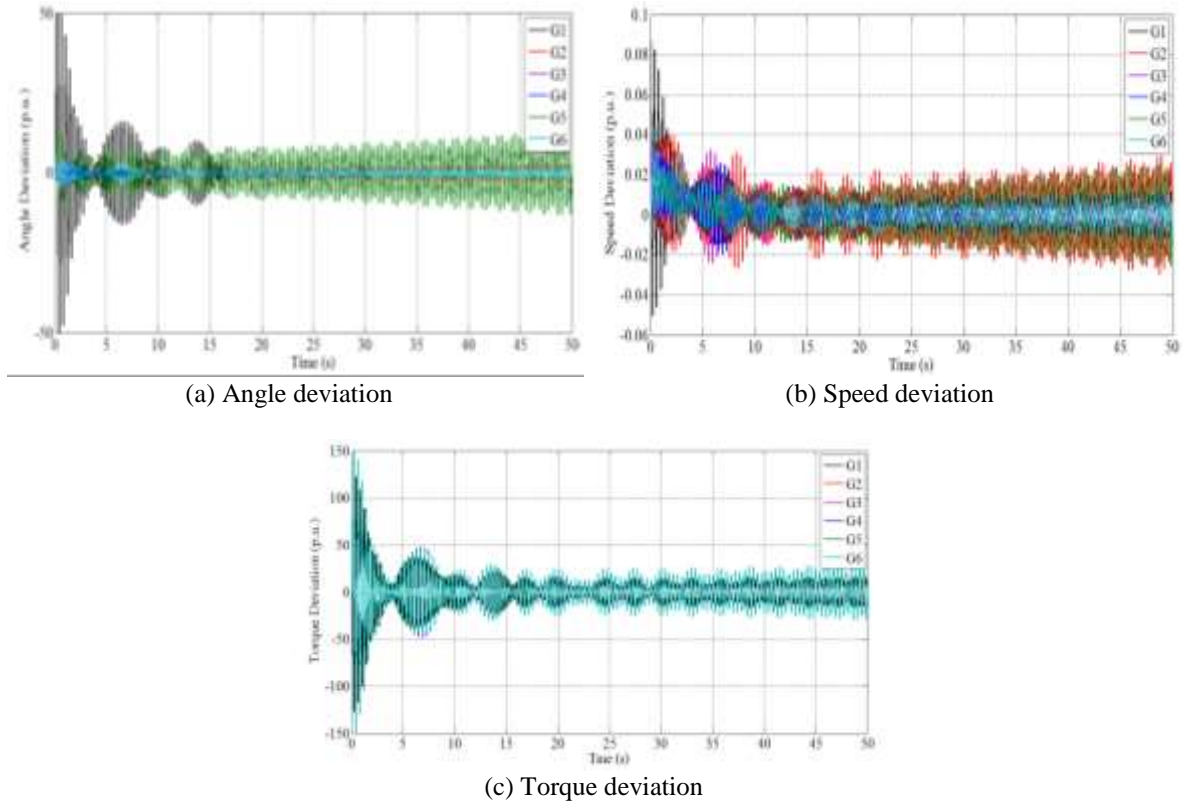


Figure 4. Responses for stable condition for all generators in case 2

The value of  $K_s$ ,  $K_d$ ,  $J$  and number of iterations for Case 2 are shown in Table 5. EP and PSO methods managed to calculate the instability conditions for Case 2 indicated by the negative results of  $K_d$  for all the six generators. On the other hand, LS failed to deliver correct results as this method calculated positive values for both  $K_s$  and  $K_d$  for generators G1 and G5. Based on this result, all the three optimization methods are highly recommended to assess the stability condition compare to LS technique. Results showed that PSO scored perfect 1.000 in fitness value at the end of the simulation process for all the six generators. EP never achieved value of 0.9 for this case. In terms of iteration number, PSO become the fastest method, followed by EP. From these results it can be said that PSO is the most capable technique in optimizing the highest quality of fitness in the calculation process with admissible computation time.

Table 5. Comparisons of EP, PSO and LS method for case 2

| Gen. | Tech. | $K_s$   | $K_d$   | $J$    | No. Iter. | Gen. | Tech. | $K_s$   | $K_d$   | $J$    | No. Iter. |
|------|-------|---------|---------|--------|-----------|------|-------|---------|---------|--------|-----------|
| G1   | EP    | 0.5182  | -0.7726 | 0.7960 | 17        | G4   | EP    | -1.1044 | -2.3948 | 0.8631 | 20        |
|      | PSO   | 0.6769  | -0.5762 | 1.0000 | 15        |      | PSO   | -0.9400 | -1.7141 | 1.0000 | 15        |
|      | LS    | 0.0730  | 0.3147  | -      | -         |      | LS    | -0.9340 | -1.0216 | -      | -         |
| G2   | EP    | 2.1324  | -1.9547 | 0.8245 | 19        | G5   | EP    | 2.1978  | -0.5515 | 0.8583 | 20        |
|      | PSO   | 2.5784  | -1.9975 | 0.9985 | 15        |      | PSO   | 2.5632  | -0.7174 | 1.0000 | 16        |
|      | LS    | 2.6721  | -1.8122 | -      | -         |      | LS    | 2.6123  | 0.0022  | -      | -         |
| G3   | EP    | -1.7429 | -2.0883 | 0.7886 | 20        | G6   | EP    | -1.1044 | -2.3947 | 0.8163 | 19        |
|      | PSO   | -1.5087 | -2.1320 | 0.9970 | 15        |      | PSO   | -0.9400 | -1.7141 | 1.0000 | 15        |
|      | LS    | -1.0877 | -1.9331 | -      | -         |      | LS    | -0.9218 | -2.0166 | -      | -         |

Table 6. The results of  $\lambda$  and  $\zeta_{min}$  for case 2

| $\zeta_{min}$ | $\lambda$                                                                                                                                                                                                                    |
|---------------|------------------------------------------------------------------------------------------------------------------------------------------------------------------------------------------------------------------------------|
| -0.0013       | -25.3894±j81.5538, -25.2323±j67.3359, -25.2296±j66.5607, -25.2493±j64.4474, -25.2044±j65.5412, -25.1783±j65.0325, -0.0014, -0.2568, 0.0184±j14.6126, -0.1184±j15.5915, -0.1250±j17.0943, -0.0364±j16.9197, -0.1278±j16.4524. |

## 5. CONCLUSION

This study has discussed the effectiveness of PSO technique in the oscillatory stability prediction in a multi-machine system. In this study, the IEEE 30-Bus test system has been selected. Although both EP and PSO are capable to predict correctly the stability condition of all cases, PSO is more convincing compared to EP. Optimization via PSO produces higher accuracy for all cases compared with EP. From the iteration point of view, PSO and EP are almost the same.

## ACKNOWLEDGEMENTS

The authors would like to acknowledge Centre for Research and Instrumentation Management (CRIM), UKM, Bangi, Selangor, Malaysia for the financial support of this research. This research is supported by Geran Galakan Penyelidik Muda (GGPM) with project code: GGPM-2018-055.

## REFERENCES

- [1] P. Kundur, *Power System Stability and Control*, New York, U.S.A: McGraw-Hill Professional, 1994.
- [2] S. Shukla and L. Mili, "Hierarchical Decentralized Control for Enhanced Rotor Angle and Voltage Stability of Large-Scale Power Systems", *IEEE Transactions on Power Systems*, Vol. 32, Issue 6, pp. 4783-4793, 2017.
- [3] H.A.M. Moussa and Y.N. Yu, "Dynamic Interaction of Multi-Machine Power System and Excitation Control", *IEEE Transactions on Power Apparatus and Systems*, Vol. PAS-93, pp. 1150-1158, 1974.
- [4] N. A. M. Kamari, I. Musirin and M. M. Othman, "Computational Intelligence Technique Based PI Controller Using SVC", *IEEE Power Engineering and Automation Conference*, 2011, pp. 354-357.
- [5] R. Yousefian, R. Bhattacharjee and S. Kamalasadan, "Transient Stability Enhancement of Power Grid with Integrated Wide Area Control of Wind Farms and Synchronous Generators", *IEEE Transactions on Power Systems*, Vol. 32, Issue 6, pp. 4818-4831, 2017.
- [6] S. Wei, M. Yang, J. Qi, J. Wang, S. Ma and X. Han, "Model-Free MLE Estimation for Online Rotor Angle Stability Assessment with PMU Data", *IEEE Transactions on Power Systems*, Vol. 33, Issue 3, pp. 2463-2476, 2018.
- [7] S. S. Refaat, H. A. Rub and A. Mohamed, "Transient Stability Impact of Large-Scale Photovoltaic System on Electric Power Grids", *IEEE Power & Energy Society Innovative Smart Grid Technologies Conference (ISGT)*, 2017, pp. 1-6.
- [8] A. Hammoudeh, M. I. Al Saaideh, E. A. Feilat and H. Mubarak, "Estimation of Synchronizing and Damping Torque Coefficients Using Deep Learning", *IEEE Jordan International Joint Conference on Electrical Engineering and Information Technology (JEEIT)*, 2019, pp. 488-493.
- [9] A. M. Yousef and A. M. Kassem, "Optimal Power System Stabilizer Based Enhancement of Synchronizing and Damping Torque Coefficients", *WSEAS Transactions on Power Systems*, Vol. 7, Issue 2, pp. 70-79, 2012.
- [10] N. A. M. Kamari, I. Musirin and M. M. Othman, "EP Based Optimization for Estimating Synchronizing and Damping Torque Coefficients", *Australian Journal of Basic and Applied Sciences*, Vol. 4, pp. 3741-3754, 2010.
- [11] M. H. M. Zaman, M. M. Mustafa and A. Hussain, "Critical Equivalent Series Resistance Estimation for Voltage Regulator Stability Using Hybrid System Identification and Neural Network", *International Journal on Advanced Science, Engineering and Information Technology*, Vol. 7, pp. 1381-1388, 2017.
- [12] S. Al-Dahidi, O. Ayadi, M. Alrbai and J. Adeeb, "Ensemble Approach of Optimized Artificial Neural Networks for Solar Photovoltaic Power Prediction", *IEEE Access*, Vol. 7, pp. 81741-81758, 2019.
- [13] Y. Sun, S. Li, B. Lin, X. Fu, M. Ramezani and I. Jaithwa, "Artificial Neural Network for Control and Grid Integration of Residential Solar Photovoltaic Systems", *IEEE Transactions on Sustainable Energy*, Vol. 8, Issue 4, pp. 1484-1495, 2017.
- [14] S. N. Annual, M. F. Ibrahim, N. Ibrahim, A. Hussain, M. M. Mustafa, A. B. Huddin and F. H. Hashim, "GA-based Optimisation of a LiDAR Feedback Autonomous Mobile Robot Navigation System", *Bulletin of Electrical Engineering and Informatics*, Vol. 7, Issue 3, pp. 433-441, 2018.
- [15] M. Yang, Y. Li, H. Du, C. Li and Z. He, "Hierarchical Multiobjective H-Infinity Robust Control Design for Wireless Power Transfer System Using Genetic Algorithm", *IEEE Transactions on Control Systems Technology*, Vol. 27, Issue 4, pp. 1753-1761, 2019.
- [16] A. A. S. Mohamed, A. Berzoy and O. A. Mohammed, "Design and Hardware Implementation of FL-MPPT Control of PV Systems Based on GA and Small-Signal Analysis", *IEEE Transactions on Sustainable Energy*, Vol. 8, Issue 1, pp. 279-290, 2017.

- [17] N. A. M. Kamari, I. Musirin and M. M. Othman, "Application of Evolutionary Programming in the Assessment of Dynamic Stability", *4th International Power Engineering and Optimization Conference (PEOCO)*, 2010, pp. 43-48.
- [18] A. F. A. Kadir, A. Mohamed, H. Shareef and M. Z. C. Wanik, "Optimal Placement and Sizing of Distributed Generations in Distribution Systems for Minimizing Losses and THD<sub>v</sub> Using Evolutionary Programming", *Turkish Journal of Electrical Engineering and Computer Sciences*, Vol. 21, pp. 2269-2282, 2013.
- [19] D. B. Mishra, A. A. Acharya and R. Mishra, "Evolutionary Algorithms for Path Coverage Test Data Generation and Optimization: A Review", *Indonesian Journal of Electrical Engineering and Computer Science*, Vol. 15, Issue 1, pp. 504-510, 2019.
- [20] L. M. Antonio and C. A. C. Coello, "Coevolutionary Multiobjective Evolutionary Algorithms: Survey of the State-of-the-Art", *IEEE Transactions on Evolutionary Computation*, Vol. 22, Issue 6, pp. 851-865, 2018.
- [21] L. E. Aik, T. W. Hong and A. K. Junoh, "An Improved Radial Basis Function Networks Based on Quantum Evolutionary Algorithm for Training Nonlinear Datasets", *IAES International Journal of Artificial Intelligence*, Vol. 8, Issue 2, pp. 120-131, 2019.
- [22] F. R. Alonso, D. Q. Oliveira and A. C. Z. De Souza, "Artificial Immune Systems Optimization Approach for Multiobjective Distribution System Reconfiguration", *IEEE Transactions on Power Systems*, Vol. 30, Issue 2, pp. 840-847, 2015.
- [23] S. C. M. Nasir, M. H. Mansor, I. Musirin, M. M. Othman, T. M. Kuan, K. Kamil and M. N. Abdullah, "Multistage Artificial Immune System for Static VAR Compensator Planning", *Indonesian Journal of Electrical Engineering and Computer Science*, Vol. 14, Issue 1, pp. 346-352, 2019.
- [24] E. Alizadeh, N. Meskin and K. Khorasani, "A Negative Selection Immune System Inspired Methodology for Fault Diagnosis of Wind Turbines", *IEEE Transactions on Cybernetics*, Vol. 47, Issue 11, pp. 3799-3813, 2017.
- [25] N. A. M. Kamari, I. Musirin, M. M. Othman and Z. A. Hamid, "PSS-LL Based Power System Stability Enhancement Using IPSO Approach", *IEEE 7th International Power Engineering and Optimization Conference (PEOCO)*, 2013, pp. 658-663.
- [26] P. Li, D. Xu, Z. Zhou, W. J. Lee and B. Zhao, "Stochastic Optimal Operation of Microgrid Based on Chaotic Binary Particle Swarm Optimization", *IEEE Transactions on Smart Grid*, Vol. 7, Issue 1, pp. 66-73, 2016.
- [27] J. S. Yang, Y. W. Chen and Y. Y. Hsu, "Small-Signal Stability Analysis and Particle Swarm Optimisation Self-Tuning Frequency Control for An Islanding System with DFIG Wind Farm", *IET Generation, Transmission & Distribution*, Vol. 13, Issue 4, pp. 563-574, 2019.
- [28] M. S. Hossain Lipu, M. A. Hannan, A. Hussain and M. H. M. Saad, "Optimal BP Neural Network Algorithm for State of Change Estimation of Lithium-Ion Battery Using PSO with PCA Feature Selection", *Journal of Renewable and Sustainable Energy*, Vol. 9, Issue 6, pp. 1-16, 2017.
- [29] H. Li, D. Yang, W. Su, J. Lü and X. Yu, "An Overall Distribution Particle Swarm Optimization MPPT Algorithm for Photovoltaic System Under Partial Shading", *IEEE Transactions on Industrial Electronics*, Vol. 66, Issue 1, pp. 265-275, 2019.
- [30] Y. Li, G. Geng, Q. Jiang, W. Li and X. Shi, "A Sequential Approach for Small Signal Stability Enhancement with Optimizing Generation Cost", *IEEE Transactions on Power Systems (Early Access)*, pp. 1-1, 2019.
- [31] M. Shafiullah, M. J. Rana and M. A. Abido, "Power System Stability Enhancement Through Optimal Design of PSS Employing PSO", *4th International Conference on Advances in Electrical Engineering (ICAEE)*, 2017, pp. 26-31.
- [32] N. A. M. Kamari, I. Musirin, Z. A. Hamid and M. N. A. Rahim, "Optimal Design of SVC-PI Controller for Damping Improvement Using New Computational Intelligence Approach", *Journal of Theoretical and Applied Information Technology*, Vol. 42, Issue 2, pp. 271-280, 2012.